

## PAPER

# Transmission Performance of Frequency-Domain Filtered Single-Carrier Transmission Using Frequency-Domain Block Signal Detection with QRM-MLD

Tetsuya YAMAMOTO<sup>†a)</sup>, Kazuki TAKEDA<sup>†</sup>, *Student Members*, KyeSan LEE<sup>††</sup>, *Member*, and Fumiyuki ADACHI<sup>†</sup>, *Fellow*

**SUMMARY** Recently, assuming ideal brick-wall transmit filtering, we proposed a frequency-domain block signal detection (FDBD) with maximum likelihood detection employing QR decomposition and M-algorithm (called QRM-MLD) for the reception of single-carrier (SC) signals transmitted over a frequency-selective fading channel. QR decomposition (QRD) is applied to a concatenation of the propagation channel and discrete Fourier transform (DFT). However, a large number of surviving paths is required in the M-algorithm to achieve sufficiently improved bit error rate (BER) performance. The introduction of filtering can achieve improved BER performance due to larger frequency diversity gain while keeping a lower peak-to-average power ratio (PAPR) than orthogonal frequency division multiplexing (OFDM). In this paper, we develop FDBD with QRM-MLD for filtered SC signal reception. QRD is applied to a concatenation of transmit filter, propagation channel, and DFT. We evaluate BER and throughput performances by computer simulation. From performance evaluation, we discuss how the filter roll-off factor affects the achievable BER and throughput performances and show that as the filter roll-off factor increases, the required number of surviving paths in the M-algorithm can be reduced.

**key words:** single-carrier, frequency-domain filtering, frequency-domain block signal detection, QRM-MLD

## 1. Introduction

Broadband data services are demanded in next generation mobile communication systems. Since the broadband channel is composed of many propagation paths with different time delays, the channel becomes severely frequency-selective [1]. The single-carrier (SC) transmission with frequency-domain equalization (FDE) has good bit error rate (BER) performance [2], [3] and low peak-to-average power ratio (PAPR) property. Therefore, the SC with FDE is advantageous for the uplink (mobile-to-base station) applications [4].

In many practical wireless systems, transmit filtering is used to limit the transmit signal bandwidth. When a square-root Nyquist filter is used, the roll-off factor  $\alpha$  ( $0 \leq \alpha \leq 1$ ) is the design parameter of the transmit filter [5]. When  $\alpha = 0$ ,

the SC signal has smaller PAPR than orthogonal frequency division multiplexing (OFDM) signal [6] while keeping the same signal bandwidth [7], [8]. As  $\alpha$  increases, the PAPR further decreases at the cost of increased bandwidth [9]. Furthermore, this increased bandwidth can be exploited to obtain larger frequency diversity gain and accordingly, improve the BER performance by using a powerful equalization scheme.

The computational complexity of the maximum likelihood (ML)-based equalization, i.e. ML sequence estimation (MLSE), depends on the number of propagation paths and becomes extremely high for a severely frequency-selective channel [10]. Therefore, several suboptimal linear detection schemes have been proposed to reduce the computational complexity. A simple one-tap FDE based on the minimum mean square error criterion (MMSE-FDE) makes use of this increased bandwidth to obtain larger frequency diversity gain and improve the BER performance [11]. However, a big performance gap from the matched-filter (MF) bound still exists due to the presence of residual inter-symbol interference (ISI) after FDE. To narrow the performance gap, an MMSE-FDE combined with iterative ISI cancellation was proposed [12]–[14]. However, the achievable BER performance is still a few dB away from the MF bound, particularly when high level data modulation (e.g., 16QAM and 64QAM) is used.

Recently, a near ML-based reduced complexity frequency-domain equalization scheme, which is called frequency-domain block signal detection (FDBD) using QR decomposition with M-algorithm ML detection (QRM-MLD), was proposed for the reception of SC signals transmitted over a frequency-selective channel [15], [16]. QRM-MLD was originally proposed in [17], [18] as a signal detection scheme for the multi-input multi-output (MIMO) spatial multiplexing. In FDBD with QRM-MLD, QR decomposition is applied to a concatenation of the propagation channel and discrete Fourier transform (DFT). We showed [16] that the FDBD with QRM-MLD can achieve the BER performance close to the MF bound while considerably reducing the computational complexity compared to the MLD. However, a large number of surviving paths is required in the M-algorithm.

It was shown [18] that by increasing the number of receive antennas, the required number of surviving paths in

Manuscript received June 3, 2010.

Manuscript revised November 15, 2010.

<sup>†</sup>The authors are with the Department of Electrical and Communication Engineering, Graduate School of Engineering, Tohoku University, Sendai-shi, 980-8579 Japan.

<sup>††</sup>The author is with the Department of Electric and Radio Engineering School of Electronics and Information, Kyung Hee University, Yongin-si Gyeonggi-do, 446-701 Republic of Korea.

a) E-mail: yamamoto@mobile.ecei.tohoku.ac.jp

DOI: 10.1587/transcom.E94.B.1386

the M-algorithm can be reduced and hence, the computational complexity of QRM-MLD can be reduced. In the case of filtered SC transmission, by viewing a concatenation of transmit filter, propagation channel, and DFT as an equivalent channel, FDBD with QRM-MLD can also be applied to the filtered SC signal reception. Larger frequency diversity gain is achieved by exploiting the excess bandwidth introduced by the transmit filter, and therefore, increasing the signal bandwidth by the transmit filter can reduce the number of surviving paths in the M-algorithm. In this paper, we develop FDBD with QRM-MLD for the reception of the filtered SC signals and investigate the BER and throughput performances by computer simulation. We discuss how the filter roll-off factor affects the achievable BER and throughput performances and the required number of surviving paths in the M-algorithm.

The remainder of this paper is organized as follows. Section 2 presents the mathematical model of frequency-domain filtered SC signal transmission using FDBD with QRM-MLD. In Sect. 3, the BER and throughput performances achievable by FDBD with QRM-MLD in a frequency-selective fading channel are evaluated by computer simulation. Section 4 offers some concluding remarks.

## 2. Frequency-Domain Filtered SC Transmission Using FDBD with QRM-MLD

### 2.1 Transmission System

The system model of the frequency-domain filtered SC signal transmission using FDBD with QRM-MLD is illustrated in Fig. 1. At the transmitter, a binary information sequence is data-modulated and then, the data-modulated symbol sequence is divided into a sequence of signal blocks  $\{d(n); n = 0 \sim N_m - 1\}$  of  $N_m$  symbols each, where  $N_m$  is the number of symbols per block. The data symbol block is transformed by  $N_m$ -point DFT into the frequency-

domain signal  $\{D(k); k = -N_m/2 \sim N_m/2 - 1\}$ , which is then, expanded to the frequency-domain signal  $\{S(k); k = -(1 + \alpha)N_m/2 \sim (1 + \alpha)N_m/2 - 1\}$  having a wider bandwidth by applying the frequency-domain transmit filter with the roll-off factor  $\alpha$ . Finally,  $N_c$ -point inverse DFT (IDFT) is applied to obtain the filtered time-domain transmit signal block  $\{s(t); t = 0 \sim N_c - 1\}$ . The last  $N_g$  samples of transmit block are copied as a cyclic prefix (CP) and inserted into the guard interval (GI) placed at the beginning of each transmit block and a CP-inserted filtered signal block of  $N_c + N_g$  samples is transmitted.

The filtered SC signal block is transmitted over a frequency-selective fading channel. The received signal block after GI removal is transformed by  $N_c$ -point DFT into the frequency-domain signal  $\{Y(k); k = -N_c/2 \sim N_c/2 - 1\}$ . Then, FDBD with QRM-MLD is carried out to obtain the decision variable block. In this paper, the discrete-time signal representation normalized by the DFT (also IDFT) sampling period  $T_c$  is used.

### 2.2 Transmit Signal Representation

The data symbol block of  $N_m$  symbols is expressed using the vector form as  $\mathbf{d} = [d(0), \dots, d(n), \dots, d(N_m - 1)]^T$ .  $\mathbf{d}$  is transformed by  $N_m$ -point DFT into the frequency-domain signal  $\mathbf{D} = [D(-N_m/2), \dots, D(k), \dots, D(N_m/2 - 1)]^T$  as

$$\mathbf{D} = \mathbf{F}^{(N_m)} \mathbf{d}, \quad (1)$$

where  $\mathbf{F}^{(J)}$  is the DFT matrix of size  $J \times J$  given by

$$\mathbf{F}^{(J)} = \frac{1}{\sqrt{J}} \begin{bmatrix} 1 & e^{-j\pi \frac{-J/2 \times 1}{J}} & \dots & e^{-j\pi \frac{-J/2 \times (J-1)}{J}} \\ 1 & e^{-j\pi \frac{(-J/2+1) \times 1}{J}} & \dots & e^{-j\pi \frac{(-J/2+1) \times (J-1)}{J}} \\ \vdots & \vdots & \ddots & \vdots \\ 1 & e^{-j\pi \frac{(J/2-1) \times 1}{J}} & \dots & e^{-j\pi \frac{(J/2-1) \times (J-1)}{J}} \end{bmatrix}. \quad (2)$$

$\mathbf{D}$  is transformed into the frequency-domain filtered signal  $\mathbf{S} = [S(-(1 + \alpha)N_m/2), \dots, S(k), \dots, S((1 + \alpha)N_m/2 - 1)]^T$  as

$$\mathbf{S} = \mathbf{H}_T \mathbf{D}, \quad (3)$$

where  $\mathbf{H}_T$  is  $(1 + \alpha)N_m \times N_m$  transmit filter matrix given by

$$\mathbf{H}_T = \begin{bmatrix} H_T(-\frac{(1+\alpha)N_m}{2}) & \mathbf{0} & & & \\ & \ddots & & & \\ & & H_T(-\frac{N_m}{2}) & \mathbf{0} & \\ & & & \ddots & \\ & & & & H_T(0) & & \\ & & & & & \ddots & \\ & & & & & & H_T(\frac{N_m}{2}) & \mathbf{0} \\ & & & & & & & \ddots & \\ \mathbf{0} & & & & & & & & H_T(\frac{(1+\alpha)N_m}{2}-1) \end{bmatrix}, \quad (4)$$

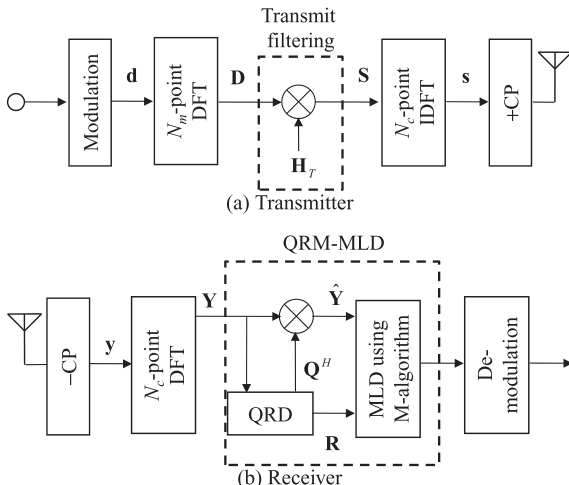


Fig. 1 System model of the frequency-domain filtered SC transmission using FDBD with QRM-MLD.

where  $H_T(k)$ ,  $k = -(1+\alpha)N_m/2 \sim (1+\alpha)N_m/2-1$ , represents the transmit filter transfer function.  $S(k)$  is given as

$$S(k) = \begin{cases} H_T(k)D(k+N_m) & -\frac{(1+\alpha)N_m}{2} \leq k \leq -\frac{N_m}{2} - 1 \\ H_T(k)D(k) & -\frac{N_m}{2} \leq k \leq \frac{N_m}{2} - 1 \\ H_T(k)D(k-N_m) & \frac{N_m}{2} \leq k \leq \frac{(1+\alpha)N_m}{2} - 1 \end{cases} \quad (5)$$

Finally,  $N_c$ -point IDFT is applied to obtain the time-domain signal block  $\mathbf{s} = [s(0), \dots, s(t), \dots, s(N_c - 1)]^T$  as

$$\mathbf{s} = \sqrt{\frac{2E_s}{T_s}} \mathbf{F}^{(N_c)^H} \tilde{\mathbf{S}}, \quad (6)$$

where  $E_s$  and  $T_s$  are respectively the transmit symbol energy and duration,  $(\cdot)^H$  is the Hermitian transpose operation, and  $\tilde{\mathbf{S}} = [\tilde{S}(-N_c/2), \dots, \tilde{S}(k), \dots, \tilde{S}(N_c/2 - 1)]^T$  given by

$$\tilde{S} = [0, \dots, 0, s(-\frac{(1+\alpha)N_m}{2}), \dots, s(k), \dots, s(\frac{(1+\alpha)N_m}{2}-1), 0, \dots, 0]^T \quad (7)$$

In this paper, IDFT at the transmitter and DFT at the receiver have the same block size  $N_c$  to keep the same sampling rate, where  $N_c \geq (1+\alpha)N_m$ , irrespective of the roll-off factor  $\alpha$  of the transmit filter (i.e. the sampling rate is always equal to  $T/N_c$ , where  $T$  is the block length excluding the cyclic prefix).

### 2.3 Received Signal Representation

We assume that the time delay of each propagation path is an integer multiple of the sampling period  $T/N_c$ . Assuming  $L$  distinct propagation paths, the channel impulse response  $h(\tau)$  can be represented as

$$h(\tau) = \sum_{l=0}^{L-1} h_l \delta(\tau - \tau_l), \quad (8)$$

where  $h_l$  and  $\tau_l$  are respectively the complex-valued path gain with  $E[\sum_{l=0}^{L-1} |h_l|^2]$  and the time delay of the  $l$ th path. We assume that the path time delay is an integer multiple of the sampling period  $T/N_c$ . The GI-removed received signal block  $\mathbf{y} = [y(0), \dots, y(t), \dots, y(N_c - 1)]^T$  can be expressed using the vector form as

$$\mathbf{y} = \sqrt{\frac{2E_s}{T_s}} \mathbf{h} \mathbf{s} + \mathbf{n}, \quad (9)$$

where  $\mathbf{h}$  is the  $N_c \times N_c$  channel impulse response matrix given as

$$\mathbf{h} = \begin{bmatrix} h_0 & & & h_{L-1} & \cdots & h_1 \\ h_1 & h_0 & & & \ddots & \vdots \\ \vdots & h_1 & h_0 & \mathbf{0} & & h_{L-1} \\ h_{L-1} & \vdots & h_1 & \ddots & & \\ & h_{L-1} & \vdots & & h_0 & \\ & & h_{L-1} & h_1 & \ddots & \\ \mathbf{0} & & & \ddots & \vdots & h_0 \end{bmatrix} \quad (10)$$

and  $\mathbf{n} = [n(0), \dots, n(t), \dots, n(N_c - 1)]^T$  is the noise vector. The  $t$ th element,  $n(t)$ , of  $\mathbf{n}$  is the zero-mean complex Gaussian variable having the variance  $2N_0/T_c$  with  $N_0$  being the one-sided power spectrum density of the additive white Gaussian noise (AWGN).

### 2.4 FDBD with QRM-MLD

The received signal block  $\mathbf{y}$  is transformed by  $N_c$ -point DFT into the frequency-domain signal  $\mathbf{Y} = [Y(0), \dots, Y(k), \dots, Y(N_c - 1)]^T$ .  $\mathbf{Y}$  is expressed as

$$\mathbf{Y} = \mathbf{F}^{(N_c)} \mathbf{y} = \sqrt{\frac{2E_s}{T_s}} \mathbf{F}^{(N_c)} \mathbf{h} \mathbf{s} + \mathbf{F}^{(N_c)} \mathbf{n}. \quad (11)$$

Due to the circulant property of  $\mathbf{h}$  [19], we have

$$\begin{aligned} \mathbf{F}^{(N_c)} \mathbf{h} \mathbf{F}^{(N_c)^H} &= \text{diag} \left[ H\left(-\frac{N_c}{2}\right), \dots, H(k), \dots, H\left(\frac{N_c}{2} - 1\right) \right] \\ &\equiv \mathbf{H}_c. \end{aligned} \quad (12)$$

where  $H(k) = \sum_{l=0}^{L-1} h_l \exp(-j2\pi k\tau_l/N_c)$ ,  $k = -N_c/2 \sim N_c/2 - 1$ .

The desired signal is present only in the frequency range of  $-(1+\alpha)N_m/2 \leq k < (1+\alpha)N_m/2$ . Therefore, the frequency-domain signal  $\tilde{\mathbf{Y}} = [\tilde{Y}(-(1+\alpha)N_m/2), \dots, \tilde{Y}(k), \dots, \tilde{Y}((1+\alpha)N_m/2 - 1)]^T$  is taken from  $\mathbf{Y}$  for FDBD with QRM-MLD.  $\tilde{\mathbf{Y}}$  can be expressed as

$$\begin{aligned} \tilde{\mathbf{Y}} &= \sqrt{\frac{2E_s}{T_s}} \tilde{\mathbf{H}}_c \mathbf{H}_T \mathbf{F}^{(N_m)} \mathbf{d} + \tilde{\mathbf{N}} \\ &= \sqrt{\frac{2E_s}{T_s}} \tilde{\mathbf{H}} \mathbf{d} + \tilde{\mathbf{N}}, \end{aligned} \quad (13)$$

where  $\tilde{\mathbf{H}}_c = \text{diag} [H(-(1+\alpha)N_m/2), \dots, H(k), \dots, H((1+\alpha)N_m/2-1)]$  and  $\tilde{\mathbf{N}} = [N(-(1+\alpha)N_m/2), \dots, N(k), \dots, N((1+\alpha)N_m/2 - 1)]^T$  is the frequency-domain noise vector.  $\tilde{\mathbf{H}} = \tilde{\mathbf{H}}_c \mathbf{H}_T \mathbf{F}^{(N_m)}$  is an equivalent channel matrix of size  $(1+\alpha)N_m \times N_m$ . It can be understood from Eq.(13) that FDBD with QRM-MLD can be applied to the frequency-domain filtered SC signal by treating a concatenation of transmit filter, frequency-domain propagation channel, and DFT as an equivalent channel.

QRM-MLD is composed of three steps. Firstly, we apply the QRD [20] to  $\tilde{\mathbf{H}}$  to obtain  $\tilde{\mathbf{H}} = \mathbf{Q}\mathbf{R}$ , where  $\mathbf{Q}$  is a  $(1+\alpha)N_m \times N_m$  matrix satisfying  $\mathbf{Q}^H \mathbf{Q} = \mathbf{I}$  ( $\mathbf{I}$  is the identity matrix) and  $\mathbf{R}$  is an  $N_m \times N_m$  upper triangular matrix. In the case of SC transmission, all symbols have the same signal-to-interference plus noise power ratio (SINR) and hence, no ordering is necessary.

Secondly, by multiplying  $\mathbf{Q}^H$  to frequency-domain received signal  $\tilde{\mathbf{Y}}$ , we have the following transformed vector

$$\hat{\mathbf{Y}} = \mathbf{Q}^H \tilde{\mathbf{Y}} = \sqrt{\frac{2E_s}{T_s}} \mathbf{R} \mathbf{d} + \mathbf{Q}^H \tilde{\mathbf{N}}. \quad (14)$$

From Eq. (14), MLD can be expressed as

$$\hat{\mathbf{d}} = \arg \min_{\mathbf{d} \in X^{N_c}} \left\| \hat{\mathbf{Y}} - \sqrt{\frac{2E_s}{T_s}} \mathbf{R} \mathbf{d} \right\|, \quad (15)$$

where  $X$  is the modulation level (e.g.,  $X = 4$  for quaternary phase shift keying (QPSK) and  $X = 16$  for 16-quadrature amplitude modulation (QAM)) and  $\bar{\mathbf{d}}$  is the candidate symbol vector.

Thirdly, MLD using the M-algorithm is carried out. Thanks to the upper triangular structure of  $\mathbf{R}$ , MLD has a tree structure of  $N_m$  stages and therefore, the M-algorithm can be applied to reduce the computational complexity. In the first stage ( $n = 0$ ), all possible symbol-candidates for the last symbol  $d(N_m - 1)$  in a data symbol block are generated (the number of all possible symbol-candidates is  $X$  for  $X$ -QAM). The path metric  $e_{n=0}$  based on the squared Euclidean distance between  $\hat{Y}(N_m - 1)$  and each symbol-candidate is computed using

$$e_{n=0} = \left| \hat{Y}(N_m - 1) - \sqrt{\frac{2E_s}{T_s}} R_{N_m-1, N_m-1} \bar{\mathbf{d}}(N_m - 1) \right|^2, \quad (16)$$

where  $\bar{\mathbf{d}}(N_m - 1)$  is the symbol-candidate for  $d(N_m - 1)$ . Next,  $M$  ( $M \leq X$ ) paths having the smallest path metric are elected as surviving paths. In the next stage ( $n = 1$ ), there are a total of  $X$  branches for  $d(N_m - 2)$  leaving from each selected surviving path. Therefore, there are a total of  $MX$  possible paths connecting two symbols,  $d(N_m - 1)$  and  $d(N_m - 2)$ . The accumulated path metric is computed for all possible  $MX$  paths using

$$e_{n=1} = \left| \hat{Y}(N_m - 2) - \sqrt{\frac{2E_s}{T_s}} \begin{pmatrix} R_{N_m-2, N_m-2} \bar{\mathbf{d}}(N_m - 2) \\ + R_{N_m-2, N_m-1} \bar{\mathbf{d}}(N_m - 1) \end{pmatrix} \right|^2 + \left| \hat{Y}(N_m - 1) - \sqrt{\frac{2E_s}{T_s}} R_{N_m-1, N_m-1} \bar{\mathbf{d}}(N_m - 1) \right|^2. \quad (17)$$

Similar to the first stage,  $M$  surviving paths are selected from  $MX$  paths. This procedure is repeated until the last stage ( $n = N_m - 1$ ). The accumulated path metric at the  $n$ th stage ( $n = 0, 1, \dots, N_m - 1$ ) is computed using

$$e_n = \sum_{n'=0}^n \left| \hat{Y}(N_m - 1 - n') - \sqrt{\frac{2E_s}{T_s}} \sum_{i=0}^{n'} R_{N_m-1-n', N_m-1-i} \bar{\mathbf{d}}(N_m - 1 - i) \right|^2. \quad (18)$$

In the uncoded transmission case, the most possible transmitted symbol sequence is found by tracing back the path having the smallest path metric at the last stage ( $n = N_m - 1$ ). In the coded transmission case, the log likelihood ratio (LLR) is used as the soft-input to the decoder. When QRM-MLD is used, however, the LLR values cannot be directly computed since  $M$  surviving paths selected at the last stage do not necessarily contain both 1 and 0 for every coded bit in a data block. In this paper, we apply the LLR estimation method proposed in [21].

The number of squared Euclidean distance computations is  $X\{1 + M(N_m - 1)\}$  for QRM-MLD and is  $X^{N_m}$  for original MLD; therefore, the number of squared Euclidean distance computations for QRM-MLD is significantly smaller than that of original MLD.

### 3. Computer Simulation

The simulation condition is shown in Table 1. We consider 16QAM data modulation,  $N_m = 64$  (the number of data symbols per block), and  $N_c = 128$  (the size of IDFT/DFT). The square-root raised cosine Nyquist filter with roll-off factor  $\alpha$  is used. The channel is assumed to be a frequency-selective block Rayleigh fading channel having  $L = 16$ -path uniform power delay profile and the normalized time delay  $\tau_l = l$ . Ideal channel estimation is assumed.

#### 3.1 BER Performance

In this paper, the channel is assumed to be composed of  $L$  independent propagation paths having time delays of an integer multiple of the sampling period  $T/N_c$ . When  $\alpha$  is small, the filter bandwidth is narrow and therefore, the delay time resolution of the receiver is low. As a consequence, the number of resolvable paths reduces and the achievable diversity order is smaller than  $L$ . On the other hand, as  $\alpha$  increases, the filter bandwidth gets wider, and therefore, the delay time resolution of the receiver improves. As a consequence, the number of resolvable paths increases and the achievable diversity order approaches  $L$ . The above discussion about the diversity order suggests that as  $\alpha$  increases, better BER performance can be achieved even if small  $M$  is used.

The average BER performance of the frequency-domain filtered SC transmission using FDBD with QRM-MLD is plotted for various values of  $M$  in Fig. 2 as a function of average received bit energy-to-noise power spectrum density ratio  $E_b/N_0 (= (E_s/N_0)(1 + N_g/N_c)/\log_2 X)$ , where  $X$  is the modulation level. For comparison, the BER performances of MMSE-FDE [11], frequency-domain iterative ISI cancellation (FDIC) [14], and the MF bound [22], [23] are also plotted. For FDIC, the use of three iterations is sufficient (i.e.,  $I = 3$ ) and therefore, only the BER performance

**Table 1** Computer simulation condition.

Transmitter	Channel code	Turbo code ( $R=1/2, 3/4, 8/9$ , and 1)
	Modulation	QPSK, 16QAM, and 64QAM
	Number of data symbols per block	$N_m=64$ symbols
	DFT/IDFT size	$N_c=128$ samples
	CP length	$N_g=16$ samples
Transmit filter	Transfer function	Square-root raised cosine
Channel	Fading type	Frequency-selective block Rayleigh
	Power delay profile	$L=16$ -path uniform power delay profile
	Time delay	$\tau_l=l$ ( $l=0-L-1$ )
Receiver	Signal detection	FDBD with QRM-MLD, MMSE-FDE, FDIC
	Channel estimation	Ideal

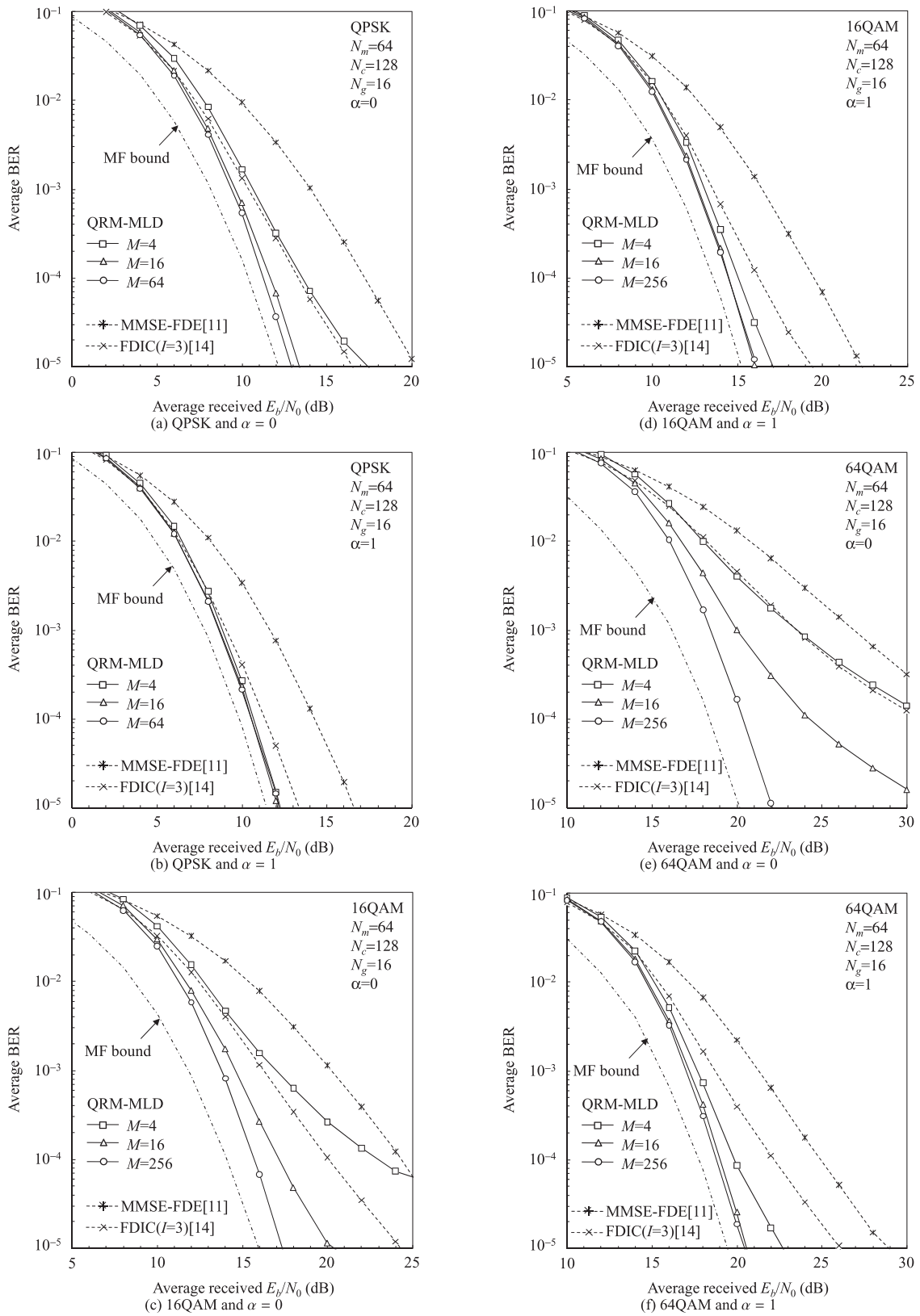


Fig. 2 BER performance (uncoded).

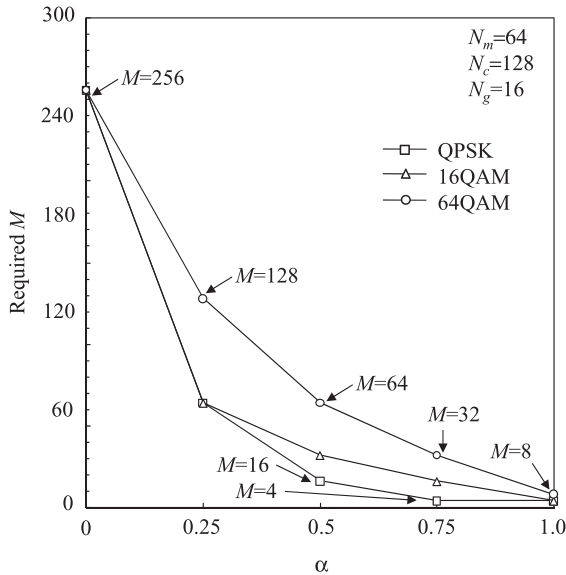


Fig. 3 Required  $M$  as a function of roll of factor  $\alpha$ .

with  $I = 3$  is plotted. It is seen from Fig. 2 that FDBD with QRM-MLD provides significantly improved BER performance compared to the MMSE-FDE. It can also be seen from Fig. 2 that FDBD with QRM-MLD provides better BER performance than FDIC. By increasing the value of  $M$ , BER performance close to the MF bound is obtained. When  $\alpha = 1$ , FDBD with QRM-MLD can reduce the average received  $E_b/N_0$  required for achieving an average BER =  $10^{-3}$  by 2.8, 3.8, and 4.0 dB for QPSK, 16QAM, and 64QAM, respectively, compared to MMSE-FDE. Compared to FDIC, FDBD with QRM-MLD can reduce the average received by 0.6, 1.0, and 2.0 dB for QPSK, 16QAM, and 64QAM, respectively.

Below, we discuss the performance gap of FDBD with QRM-MLD from the MF bound in terms of  $E_b/N_0$  required for achieving an average BER =  $10^{-3}$ . When  $\alpha = 0$ ,  $E_b/N_0$  gap with  $M = 256$  is found to be 1.2, 1.8, and 2.0 dB for QPSK, 16QAM, and 64QAM, respectively. As  $\alpha$  increases, the required  $M$  can be reduced if we want to keep the same  $E_b/N_0$  gap as shown above. Figure 3 plots the required  $M$  as a function of  $\alpha$ . When  $\alpha = 1$ , much smaller  $M$  can be used;  $M = 4$  for QPSK and 16QAM and  $M = 8$  for 64QAM. This suggests that increasing  $\alpha$  can significantly reduce the computational complexity of FDBD with QRM-MLD. The computational complexity comparison among FDBD with QRM-MLD, MMSE-FDE, and FDIC will be discussed in the next subsection.

Below, assuming 16QAM data modulation, we compare the coded BER performances of FDBD with QRM-MLD, MMSE-FDE, and FDIC. Rate-1/3 turbo coding using two (13, 15) recursive systematic convolutional (RSC) component encoders is assumed. The two parity sequences from the turbo encoder are punctured to obtain rate-1/2, 3/4, and 8/9 turbo codes. Log-MAP decoding with 6 iterations is performed after signal detection for FDBD with QRM-MLD

and MMSE-FDE. On the other hand, when FDIC is used, a series of channel decoding, equalization, and ISI cancellation is performed in an iterative fashion (called MMSE turbo equalization in this paper) [24], [25] and the number of iterations,  $I$ , in the MMSE turbo equalization is assumed to be  $I = 6$ . The packet length is set to 8 blocks ( $8 N_m$  symbols) in all simulations.

The BER performance of turbo coded frequency-domain filtered SC transmission using FDBD with QRM-MLD is plotted in Fig. 4 as a function of average received  $E_b/N_0 (= R(E_s/N_0)(1 + N_g/N_c)/\log_2 X)$ . For comparison, the BER performances of MMSE-FDE and MMSE turbo equalization are also plotted. It can be seen from Fig. 4 that when  $\alpha = 1$ , as in the uncoded case, better BER performance can be achieved even if small  $M$  is used. It can also be seen from Fig. 4 that FDBD with QRM-MLD provides much better BER performance than MMSE-FDE and slightly better BER performance than MMSE turbo equalization when high-rate turbo coding is used. When  $R = 8/9$  and  $\alpha = 0(1)$ , FDBD with QRM-MLD using  $M = 16$  can reduce the  $E_b/N_0$  value required for achieving an average BER =  $10^{-3}$  by about 3.5(2.0) dB compared to MMSE-FDE and by about 1.0(0.5) dB compared to MMSE turbo equalization. On the other hand, when low-rate turbo coding is used, FDBD with QRM-MLD provides almost the same BER performance as MMSE turbo equalization.

### 3.2 Complexity

The computational complexity of FDBD with QRM-MLD is discussed. The complexity here is defined as the number of complex multiply operations per data symbol block. First, we examine the number of multiply operations required for squared Euclidean distance computation. From Eq. (18), the number of multiply operations at the  $n$ th stage ( $n = 0 \sim N_m - 1$ ) in the M-algorithm is  $MX(n + 2)$ . Therefore, the number of multiply operations required for squared Euclidean distance computation is a function of  $M$  and is  $X\{2 + (M/2)(N_m + 4)(N_m - 1)\}$ . As  $\alpha$  increases, the required value of  $M$  can be reduced (see Fig. 3) and therefore, the complexity required for squared Euclidean distance computation can also be reduced. When  $\alpha = 1$ , it can be about 1.6% of the case of  $\alpha = 0$  for 16QAM.

Next, we discuss the overall computational complexity, (defined as a sum of the complexities required for DFT, QR decomposition,  $\mathbf{Q}^H$  multiplication, and squared Euclidean distance computation). The number of complex multiply operations is  $J^2$  for  $J$ -point DFT,  $(1 + \alpha)N_m^3$  for QR decomposition, and  $(1 + \alpha)N_m^2$  for  $\mathbf{Q}^H$  multiplication. As  $\alpha$  increases, the complexity significantly reduces for squared Euclidean computation, while it gets higher for QR decomposition and  $\mathbf{Q}^H$  multiplication. As a result, the overall complexity reduces as  $\alpha$  increases. For the uncoded case using 16QAM, the complexity when  $\alpha = 1.0$  is about 7.6% of that when  $\alpha = 0$ .

Finally, we compare the overall computational complexities of FDBD with QRM-MLD, MMSE-FDE, and

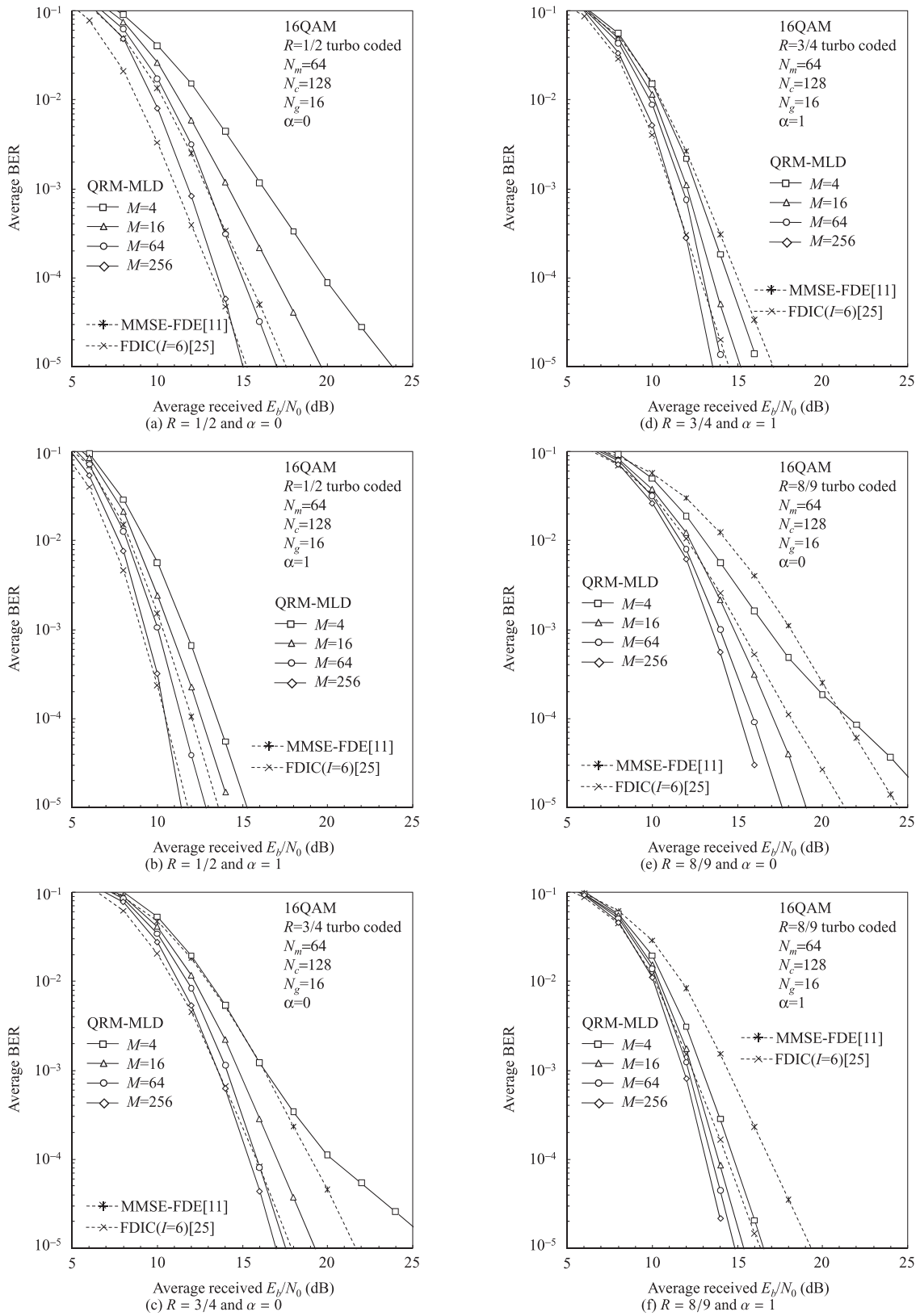
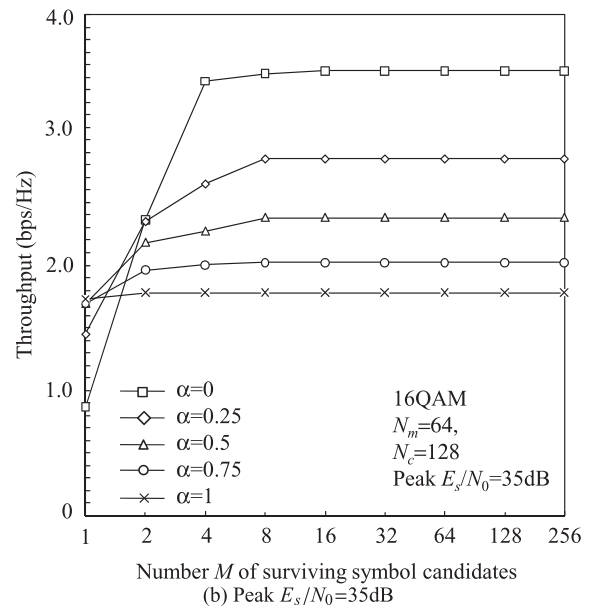
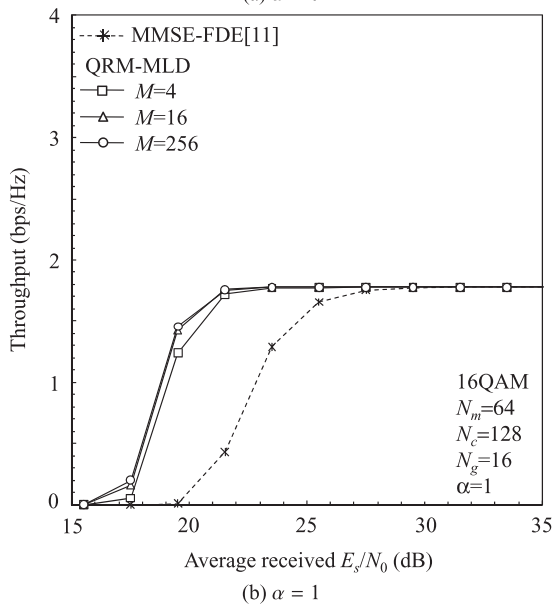
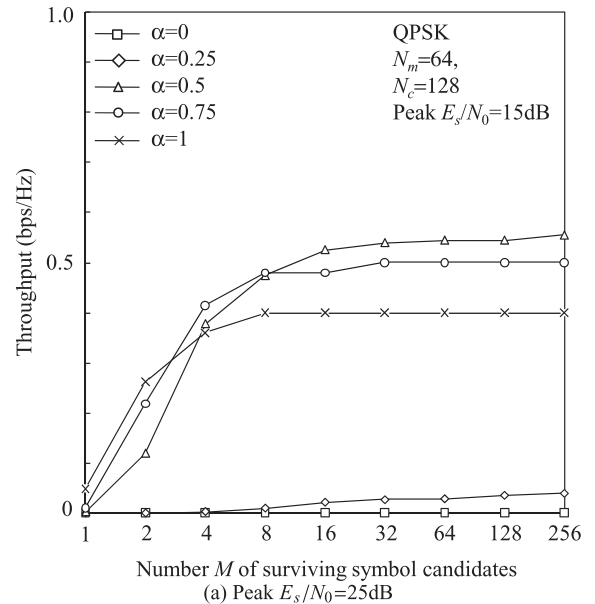
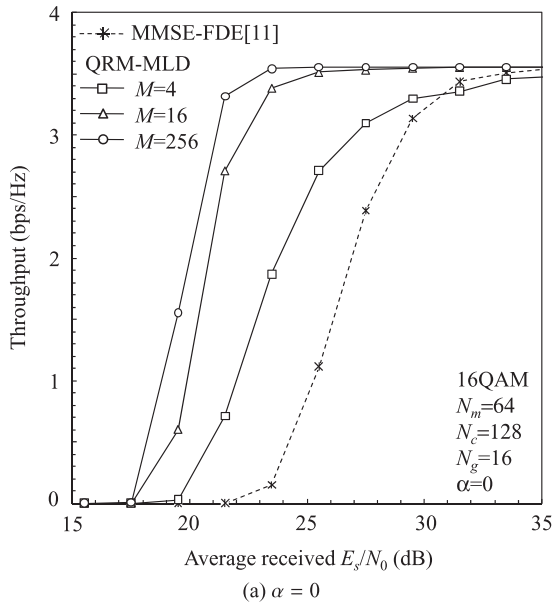


Fig. 4 BER performance (turbo coded).

**Table 2** Number of multiply operations per block.

	FDBD with QRM-MLD	MMSE-FDE	FDIC
FFT/IFFT	$N_c^2$	$N_c^2 + N_m^2$	$N_c^2 + (I+1)N_m^2$
QR decomposition/Weight computation	$(1+\alpha)N_m^3$	$(1+\alpha)N_m$	$(I+1)(1+\alpha)N_m$
$\mathbf{Q}^H$ multiplication/Weight multiplication	$(1+\alpha)N_m^2$	$(1+\alpha)N_m$	$(I+1)(1+\alpha)N_m$
Squared Euclidian distance computation /Replica generation (including LLR calculation)	$X\{2+(M/2)(N_m+4)(N_m-1)\}$	$2(3+\alpha+X)N_m+1$	$I\{N_m^2+(9+2\alpha+2X)N_m+1\}$ $+2(3+\alpha+X)N_m+1$



**Fig. 5** Throughput performance.

**Fig. 6** Throughput versus number  $M$  of surviving symbol candidates in the  $M$ -algorithm.

FDIC. The number of complex multiply operations per data symbol block is shown in Table 2. FDBD with QRM-MLD can achieve better BER performance than MMSE-FDE and FDIC at the cost of higher complexity. Its complexity is about 30 times and 14 times higher than MMSE-FDE and

FDIC, respectively for the uncoded case using  $\alpha = 1.0$ ,  $N_m = 64$ , and 16QAM.

### 3.3 Throughput Performance

The throughput performance is plotted for various values of  $M$  in Fig. 5 as a function of average received  $E_s/N_0$ . Uncoded transmission and 16QAM are assumed. The throughput  $\eta$ (bps/Hz) is defined as

$$\eta = \log_2 X \times (1 - PER) \times \frac{1}{1 + \alpha} \times \frac{1}{1 + N_g/N_c}, \quad (19)$$

where PER is the packet error rate. In this paper, packet transmission of size 1024 bits is assumed. For comparison, the throughput performance using MMSE-FDE [11] is also plotted in Fig. 5. FDBD with QRM-MLD can significantly improve the throughput performance compared to the MMSE-FDE. Furthermore, by increasing the value of  $M$ , sufficiently improved throughput performance is achieved. Furthermore, as  $\alpha$  increases, sufficiently improved throughput performance can be achieved even if small  $M$  is used.

Figure 6 plots the throughput as a function of  $M$  when the peak  $E_s/N_0 = 25$  dB and 35 dB. Peak  $E_s/N_0$  is defined as the average received  $E_s/N_0$  plus  $PAPR_{0.1\%}$  value (note that  $PAPR_{0.1\%}$  value is taken from [11]). As  $\alpha$  increases, smaller  $M$  is required to achieve sufficiently improved throughput. It can also be seen from Fig. 6 that in low peak  $E_s/N_0$  region (peak  $E_s/N_0 = 25$  dB), when  $M$  is smaller than 4, the throughput increases as  $\alpha$  increases and the maximum throughput is obtained when  $\alpha = 1$ . This is because by increasing  $\alpha$ , larger frequency diversity gain can be obtained. On the other hand, when  $M$  is large enough (e.g.,  $M \geq 16$ ), the throughput is maximized when  $\alpha = 0.5$ . This is because when  $M$  is large enough, sufficiently improved throughput can be achieved even when  $\alpha$  is small, however, the PAPR level becomes almost the same beyond  $\alpha = 0.5$ . However, in a high  $E_s/N_0$  region (peak  $E_s/N_0 = 35$  dB), increasing  $\alpha$  reduces the throughput due to increased bandwidth.

### 4. Conclusion

In this paper, we developed a computational efficient FDBD with QRM-MLD for filtered SC signal reception. QRD is applied to a concatenation of transmit filter, propagation channel, and DFT. We showed that FDBD with QRM-MLD can significantly improve the BER and throughput performances compared to the MMSE-FDE. Furthermore, we showed that as  $\alpha$  increases, better BER performance can be achieved even if small  $M$  is used. As a result, by increasing  $\alpha$ , the computational complexity of FDBD with QRM-MLD can be reduced at the cost of increased bandwidth. We also showed that in the low peak  $E_s/N_0$  region, when  $M$  is small, the throughput increases as  $\alpha$  increases and the maximum throughput is obtained when  $\alpha = 1$ . On the other hand, when  $M$  is large enough, the throughput is maximized when  $\alpha = 0.5$ .

In this paper, we examined the frequency-domain QRM-MLD assuming a block fading channel (very weak time-selectivity). If the channel time-selectivity is strong,

the frequency-domain channel matrix is not any more diagonal. FDBD with QRM-MLD in a time-selective channel is left as an important future topic. It should be noted that QRM-MLD can also be applied to the time-domain received signal. Time-domain block signal detection with QRM-MLD is left as another important future topic. In this paper, we investigated the transmission performance in a single-user environment. When we apply the FDBD with QRM-MLD to a multi-user environment, the signal spectra of adjacent users overlap if the carrier frequency separation is kept the same as in the case of  $\alpha = 0$ . This produces a large multi-user interference (MUI) and significantly degrades the BER and throughput performances. A multi-user FDBD with QRM-MLD is left as an important future study topic.

### References

- [1] J.G. Proakis and M. Salehi, Digital communications, 5th ed., McGraw-Hill, 2008.
- [2] D. Falconer, S.L. Ariyavisitakul, A. Benyamin-Seeyar, and B. Edison, "Frequency domain equalization for single-carrier broadband wireless systems," IEEE Commun. Mag., vol.40, no.4, pp.58–66, April 2002.
- [3] F. Adachi, T. Sao, and T. Itagaki, "Performance of multicode DS-SS using frequency domain equalization in a frequency selective fading channel," Electron. Lett., vol.39, no.2, pp.239–241, Jan. 2003.
- [4] H. Ekstrom, A. Furuskar, J. Karlsson, M. Meyer, S. Park-vall, J. Torsner, and M. Wahlqvist, "Technical solutions for the 3G long-term evolution," IEEE Commun. Mag., vol.44, no.3, pp.38–45, March 2006.
- [5] R. Van Nee and R. Prasad, OFDM for Wireless Multimedia Communications, Artech House, 2000.
- [6] Y. Akaiwa, Introduction to digital mobile communication, Wiley, New York, 1997.
- [7] H.G. Myung and D.J. Goodman, Introduction to single carrier FDMA: A new air interface for long term evolution, John Wiley & Sons, 2008.
- [8] V. Tarokh and H. Jafarkhani, "On the computation and reduction of the per-to-average power ratio in multicarrier communications," IEEE Trans. Commun., vol.48, no.1, pp.37–44, Jan. 2000.
- [9] S. Daumont, B. Rihawi, and Y. Lout, "Root-raised cosine filter influences on PAPR distribution of single carrier signals," 2nd International Symposium on Communications, Control and Signal Processing (ISCCSP 2008), pp.841–845, Malta, March 2008.
- [10] G.D. Forney, Jr., "Maximum likelihood sequence estimation of digital sequence in the presence of intersymbol interference," IEEE Trans. Inf. Theory, vol.18, no.3, pp.363–378, May 1972.
- [11] S. Okuyama, K. Takeda, and F. Adachi, "MMSE frequency-domain equalization using spectrum combining for Nyquist filtered broadband single-carrier transmission," 71st Vehicular Technology Conference (VTC2010-Spring), Taiwan, May 2010.
- [12] N. Benvenuto and S. Tomasin, "Block iterative DFE for single carrier modulation," Electron. Lett., vol.38, no.19, pp.1144–1145, Sept. 2002.
- [13] S. Tomasin and N. Benvenuto, "Iterative design and detection of a DFE in the frequency domain," IEEE Trans. Commun., vol.53, no.11, pp.1867–1875, Nov. 2005.
- [14] K. Takeda, K. Ishihara, and F. Adachi, "Frequency-domain ICI cancellation with MMSE equalization for DS-SS downlink," IEICE Trans. Commun., vol.E89-B, no.12, pp.3335–3343, Dec. 2006.
- [15] K. Nagatomi, K. Higuchi, and H. Kawai, "Complexity reduced MLD based on QR decomposition in OFDM MIMO multiplex-

ing with frequency domain spreading and code multiplexing,” Proc. IEEE Wireless Communications and Networking Conference (WCNC 2009), pp.1–6, April 2009.

- [16] T. Yamamoto, K. Takeda, and F. Adachi, “Single-carrier transmission using QRM-MLD with antenna diversity,” 12th International Symposium on Wireless Personal Multimedia Communications (WPMC 2009), Japan, Sept. 2009.
- [17] L.J. Kim and J. Yue, “Joint channel estimation and data detection algorithms for MIMO-OFDM systems,” Proc. 36th Asilomar Conference on Signals, System and Computers, pp.1857–1861, Nov. 2002.
- [18] K. Higuchi, H. Kawai, N. Maeda, and M. Sawahashi, “Adaptive Selection of Surviving Symbol Replica Candidates Based on Maximum Reliability in QRM-MLD for OFCDM MIMO Multiplexing,” Proc. IEEE Globecom 2004, pp.2480–2486, Nov. 2004.
- [19] G.H. Golub and C.F. van Loan, *Matrix Computations*, 3rd ed. Johns Hopkins Univ. Press, Baltimore, MD, 1996.
- [20] J. Morale-Jimenez, F. Paris, and, J.T. Entrambasaguas, “Performance tradeoff among low-complexity detection algorithm for MIMO-LTE receivers,” *Int. J. Commun. Syst.*, vol.22, no.7, pp.885–897, July 2009.
- [21] W. Shin, H. Kim, M. Son, and H. Park, “An improved LLR computation for QRM-MLD in coded MIMO systems,” Proc. IEEE 66th Vehicular Technology Conference (VTC2007-Fall), pp.447–451, Sept., Oct. 2007.
- [22] F. Adachi and K. Takeda, “Bit error rate analysis of DS-CDMA with joint frequency-domain equalization and antenna diversity combining,” *IEICE Trans. Commun.*, vol.E87-B, no.10, pp.2991–3002, Oct. 2004.
- [23] K. Takeda and F. Adachi, “Frequency-interleaved spread spectrum with MMSE frequency-domain equalization,” *IEICE Trans. Commun.*, vol.E90-B, no.2, pp.260–268, Feb. 2007.
- [24] X. Wang and H.V. Poor, “Iterative (turbo) soft interference cancellation and decoding for coded CDMA,” *IEEE Commun. Mag.*, vol.47, no.7, pp.1046–1060, July 1999.
- [25] C. Laot, R.L. Bidan, and D. Leroux, “Low-complexity MMSE turbo Equalization: A possible solution for EDGE,” *IEEE Trans. Wirel. Commun.*, vol.4, no.3, pp.965–974, May 2005.



**Tetsuya Yamamoto** received his B.S. degree in Electrical, Information and Physics Engineering in 2008 and M.S. degree in communications engineering, in 2010, respectively, from Tohoku University, Sendai Japan. Currently he is a Japan Society for the Promotion of Science (JSPS) research fellow, studying toward his Ph.D. degree at the Department of Electrical and Communications Engineering, Graduate School of Engineering, Tohoku University. His research interests include frequency-domain equalization

and signal detection techniques for mobile communication systems. He was a recipient of the 2008 IEICE RCS (Radio Communication Systems) Active Research Award.



**Kazuki Takeda** received his B.S., M.S., and Dr. Eng. degrees in communications engineering from Tohoku University, Sendai, Japan, in 2006, 2008, and 2010, respectively. Currently he is a Japan Society for the Promotion of Science (JSPS) research fellow at the Department of Electrical and Communication Engineering, Graduate School of Engineering, Tohoku University. His research interests include precoding and channel equalization techniques for mobile communication systems. He was a recipient of

the 2009 IEICE RCS (Radio Communication Systems) Active Research Award.



**KyeSan Lee** received a B.E. degree in electrical engineering from Kyung Hee University in Korea and M.S. and Ph.D. degrees from the department of electrical engineering, Keio University, Yokohama, Japan, in 1996, 1999, and 2002, respectively. He joined KDDI R&D Laboratories Inc. in 2002 and has received an IEEE VTS Japan young researchers encouragement award. Since 2003, he has been with the College of Electronic and Information, Kyung Hee University, where he is a Professor. His research

interests include wireless communication network, CDMA, OFDM, MC-CDMA, MIMO, and Cognitive radio and Visible Light Communication systems.



**FumiYuki Adachi** received the B.S. and Dr. Eng. degrees in electrical engineering from Tohoku University, Sendai, Japan, in 1973 and 1984, respectively. In April 1973, he joined the Electrical Communications Laboratories of Nippon Telegraph & Telephone Corporation (now NTT) and conducted various types of research related to digital cellular mobile communications. From July 1992 to December 1999, he was with NTT Mobile Communications Network, Inc. (now NTT DoCoMo, Inc.), where he

led a research group on wideband/broadband CDMA wireless access for IMT-2000 and beyond. Since January 2000, he has been with Tohoku University, Sendai, Japan, where he is a Professor of Electrical and Communication Engineering at the Graduate School of Engineering. His research interests are in CDMA wireless access techniques, equalization, transmit/receive antenna diversity, MIMO, adaptive transmission, and channel coding, with particular application to broadband wireless communications systems. From October 1984 to September 1985, he was a United Kingdom SERC Visiting Research Fellow in the Department of Electrical Engineering and Electronics at Liverpool University. He was a co-recipient of the IEICE Transactions best paper of the year award 1996 and again 1998 and also a recipient of Achievement award 2003. He is an IEEE Fellow and was a co-recipient of the IEEE Vehicular Technology Transactions best paper of the year award 1980 and again 1990 and also a recipient of Avant Garde award 2000. He was a recipient of Thomson Scientific Research Front Award 2004, Ericsson Telecommunications Award 2008, Telecom System Technology Award 2009, and Prime Minister Invention Prize 2010.